Check for updates

Ultrasound Obstet Gynecol 2023; **62**: 860–866
Published online in Wiley Online Library (wileyonlinelibrary.com). **DOI:** 10.1002/uog.26312.
This is an open access article under the terms of the Creative Commons Attribution-NonCommercial-NoDerivs License, which permits use and distribution in any medium, provided the original work is properly cited, the use is non-commercial and no modifications or adaptations are made.

Longitudinal assessment of spiral and uterine arteries in normal pregnancy using novel ultrasound tool

R. HORGAN[1], E. SINKOVSKAYA[1], G. SAADE[2], E. KALAFAT[3], M. M. RICE[4], A. HEEZE[1] and A. ABUHAMAD[1]

[1]*Division of Maternal–Fetal Medicine, Department of Obstetrics and Gynecology, Eastern Virginia Medical School, Norfolk, VA, USA;* [2]*Division of Maternal–Fetal Medicine, Department of Obstetrics and Gynecology, University of Texas Medical Branch, Galveston, TX, USA;* [3]*Department of Obstetrics and Gynecology, Koc University School of Medicine, Istanbul, Turkey;* [4]*George Washington University Biostatistics Center, Milken Institute School of Public Health, Washington, DC, USA*

KEYWORDS: Doppler; placenta; spiral artery; superb microvascular imaging; uterine artery

CONTRIBUTION

What are the novel findings of this work?
In this study, we assessed the use of superb microvascular imaging to evaluate longitudinally spiral and uterine artery vascular adaptation in normal human pregnancy, and developed reference ranges for use between 12 and 38 weeks' gestation. We noted a close correlation between the changes in Doppler indices of the uterine artery and the spiral artery in normal pregnancy.

What are the clinical implications of this work?
We have demonstrated the ability to assess non-invasively the human placenta throughout pregnancy using superb microvascular imaging. We present reference ranges for maternal placental vasculature from the first to third trimester in order to facilitate identification of pregnancies affected by abnormal uterine vascular adaptation.

ABSTRACT

Objectives *To use superb microvascular imaging (SMI) to evaluate longitudinally spiral artery (SA) and uterine artery (UtA) vascular adaptation in normal human pregnancy, and to develop reference ranges for use at various gestational ages throughout pregnancy.*

Methods *The data for this study were obtained from the National Institutes of Health (NIH)-funded Human Placenta Project. Women aged 18–35 years, with a body mass index < 30 kg/m^2, without comorbidities, with a singleton gestation conceived spontaneously, and gestational age at or less than 13 + 6 weeks were eligible for inclusion. The current analysis was restricted to uncomplicated pregnancies carried to term. Exclusion criteria included maternal or neonatal complications, fetal or umbilical cord anomalies, abnormal placental implantation or delivery < 37 weeks. Women who fulfilled the inclusion criteria formed the reference population of the Human Placenta Project study. Each participant underwent eight ultrasound examinations during pregnancy. The pulsatility index (PI) of both the left and right UtA were obtained twice for each artery and the presence or absence of a notch was noted. Using SMI technology, the total number of SA imaged was recorded in a sagittal placental section at the level of cord insertion. The PI and peak systolic velocity (PSV) were also measured in a total of six SA, including two in the central portion of the placenta, two peripherally towards the uterine fundal portion, and two peripherally towards the lower uterine segment.*

Results *A total of 90 women fulfilled the study criteria. Maternal UtA-PI decreased throughout the first half of pregnancy from a mean ± SD of 1.39 ± 0.50 at 12–13 weeks' gestation to 0.88 ± 0.24 at 20–21 weeks' gestation. The mean number of SA visualized in a sagittal plane of the placenta increased from 8.83 ± 2.37 in the first trimester to 16.99 ± 3.31 in the late-third trimester. The mean SA-PI was 0.57 ± 0.12 in the first trimester and decreased progressively during the second trimester, reaching a nadir of 0.40 ± 0.10 at 24–25 weeks, and remaining constant until the end of pregnancy. SA-PSV was highest in early pregnancy with a mean of 57.16 ± 14.84 cm/s at 12–13 weeks' gestation, declined to a mean of 49.38 ± 17.88 cm/s at 20–21 weeks' gestation*

Correspondence to: Dr R. Horgan, Division of Maternal–Fetal Medicine, Department of Obstetrics and Gynecology, Eastern Virginia Medical School, 825 Fairfax Avenue, Suite 528, Norfolk, VA 23507, USA (e-mail: horganr@evms.edu)

Accepted: 22 June 2023

© 2023 The Authors. *Ultrasound in Obstetrics & Gynecology* published by John Wiley & Sons Ltd on behalf of International Society of Ultrasound in Obstetrics and Gynecology.

and continued to trend downward for the remainder of pregnancy, reaching a nadir of 34.50 ± 15.08 cm/s at 36–37 weeks' gestation. A statistically significant correlation was noted between SA-PI and UtA-PI (r = 0.5633; P < 0.001). Multilevel regression models with natural cubic splines were used to create reference ranges of SA-PSV and SA-PI for given gestational ages.

Conclusion *From early gestation, we have demonstrated the ability to image and quantify SA blood flow in normal pregnancy, and have developed reference ranges for use at various gestational ages throughout pregnancy.* © *2023 The Authors. Ultrasound in Obstetrics & Gynecology published by John Wiley & Sons Ltd on behalf of International Society of Ultrasound in Obstetrics and Gynecology.*

INTRODUCTION

Maternal spiral arteries (SAs) arise from branches of the uterine arteries (UtAs). Vascular remodeling of the SAs is recognized as a critical step in pregnancy adaptation, which is thought to ensure adequate perfusion to the placenta and the developing fetus. Early in gestation, extravillous cytotrophoblasts invade the media and endothelium of the SA vessel walls, resulting in replacement of the muscular component of the vascular wall with inelastic fibrinoid material, ensuring a stable blood supply to the placental intervillous spaces[1,2].

Abnormal development of the placenta is believed to be the underlying pathogenesis for many adverse pregnancy outcomes[3]. In such abnormal development, placental histopathology demonstrates shallow extravillous trophoblast invasion with incomplete maternal spiral vessel remodeling, resulting in high-impedance, low-capacity vessels. This placental malperfusion is demonstrated further by decreased villous volume and fibrin deposition, enhanced trophoblast apoptosis and denudation of the villous syncytiotrophoblast layer on placental histopathology[3,4]. Although high impedance of the UtAs is associated with fetal growth restriction (FGR), UtA Doppler indices have relatively low sensitivity for prediction of FGR. Therefore, the possibility of directly assessing blood flow at the uteroplacental interface rather than in the upstream UtA has been proposed as a possible method to improve the accuracy of predicting adverse pregnancy outcome[5]. Previous work has suggested that direct evaluation of the SAs is reliable, reproducible and a potentially useful tool to assess risk for adverse pregnancy outcome[5–8].

Until recently, we have been unable to accurately assess placental microvasculature due to limitations in ultrasound technology. Superb microvascular imaging (SMI) is a novel Doppler technique designed to improve the visualization of microscopic vessels through a new adaptive algorithm that can separate low-velocity weak flow signals from overlying tissue motion artifacts, and display microvascular flow without the need for contrast agents[9–13]. To further assess the potential utility of SA assessment in the prediction of abnormal pregnancy outcomes, knowledge of normal values is essential.

The primary objective of this study was to use SMI to evaluate longitudinally SA and UtA vascular adaptation in normal human pregnancy, and to develop reference ranges for its use at various gestational ages throughout pregnancy.

METHODS

The data for this study were obtained from the large Human Placenta Project database (study: HD 086313-01) and additional data points were collected at each ultrasound examination as per the National Institutes of Health (NIH) study protocol. Women registered for prenatal care at Eastern Virginia Medical School (EVMS), Norfolk, VA, USA, from January 2016 to March 2020 were invited to participate. Women aged 18–35 years, with a body mass index < 30 kg/m^2, without comorbidities, with a singleton gestation conceived spontaneously and gestational age at or less than 13 + 6 weeks were eligible for inclusion. The current analysis was restricted to uncomplicated pregnancies carried to term. Exclusion criteria included maternal or neonatal complications, fetal or umbilical cord anomalies, abnormal placental implantation or delivery < 37 weeks. Abnormal placental implantation and umbilical cord abnormalities were defined as placenta previa (covering the internal cervical os), bilobed placenta, and marginal or velamentous cord insertion at the time of recruitment in the first trimester.

Women who fulfilled the inclusion criteria were considered to have a normal pregnancy, with normal maternal and neonatal outcome, and formed the reference population of the Human Placenta Project study. Written consent was obtained from all participants prior to participation. The study received approval from the Institutional Review Board of EVMS. The maternal–fetal medicine ultrasound unit at EVMS is accredited by the American Institute of Ultrasound in Medicine (AIUM) for various obstetric ultrasound examinations to include the first- and second-trimester ultrasound. The As Low As Reasonably Achievable (ALARA) Principle and ultrasound safety considerations were adhered to at all times.

Ultrasound examinations commenced between 12 + 0 and 13 + 6 weeks and were performed every 2 weeks until 16 weeks' gestation, then every 4 weeks until 38 weeks, for a total of eight longitudinal ultrasound examinations per pregnancy. The gestational-age windows for the eight ultrasound examinations were as follows: 12 + 0 to 13 + 6; 14 + 0 to 15 + 6; 16 + 0 to 17 + 6; 20 + 0 to 21 + 6; 24 + 0 to 25 + 6; 28 + 0 to 29 + 6; 32 + 0 to 33 + 6; and 36 + 0 to 37 + 6 weeks' gestation. All measurements were performed transabdominally using Toshiba AplioTM i500/Canon AplioTM i800 ultrasound systems with an i8Cx1 convex transducer (Canon Medical Corp., Tochigi, Japan). Sonographers performing the ultrasound examinations were trained in the application of SMI and had to pass a quality assurance review of five ultrasound examinations before participating in the study. All ultrasound measurements were also independently reviewed remotely by two examiners to ensure quality.

© 2023 The Authors. *Ultrasound in Obstetrics & Gynecology* published by John Wiley & Sons Ltd on behalf of International Society of Ultrasound in Obstetrics and Gynecology.

14690705, 2023, 6, Downloaded from https://obgyn.onlinelibrary.wiley.com/doi/10.1002/uog.26312 by Koc University, Wiley Online Library on [26/02/2024]. See the Terms and Conditions (https://onlinelibrary.wiley.com/terms-and-conditions) on Wiley Online Library for rules of use; OA articles are governed by the applicable Creative Commons License

The remainder of prenatal care was at the discretion of the healthcare team.

SA assessment using SMI technology was performed as per techniques described previously[8,14]. In summary, maternal SA were imaged in a longitudinal section of the placenta, at the level of the cord insertion (Figure 1). The opening of the SA was identified at the point it opens into the intravillous space on the maternal side of the placenta and further identified by their characteristic waveform pattern. SAs were differentiated from other placental vasculature by their location just beneath the placenta. SAs were assessed based on their location within the placenta: centrally, and peripherally towards the fundus of the uterus or the lower segment. The width of the cord insertion into the placenta was used in designating the location of SA, with central location defined as three cord widths around the cord insertion, and peripherally as outside this region, towards the fundus (fundally) and towards the lower segment (lower segment). There was no difference in SA-PI or -PSV based on sampling location within the placenta. Therefore, mean SA-PI and -PSV for each patient was calculated by averaging the six associated measurements for both SA-PSV and -PI (central, lower and fundal).

UtA Doppler measurements were assessed according to the International Society of Ultrasound in Obstetrics and Gynecology (ISUOG) guidelines[15], by obtaining a midsagittal section of the uterus and locating the main branch of the UtA at the cervicocorporeal junction. Measurements of both the right and left UtA were then obtained at the point before the UtA branches into the arcuate arteries with the PI of both the left and right UtA obtained twice for each artery and the presence or absence of a notch noted[15]. Notching was defined qualitatively as reduced early diastolic velocity before the maximum diastolic velocity in the Doppler waveform, in accordance with ISUOG guidelines[15]. The average PI of the right and left UtAs was calculated. Using SMI technology, the total number of SA imaged was recorded in a sagittal placental section at the level of cord insertion and PI and PSV were measured.

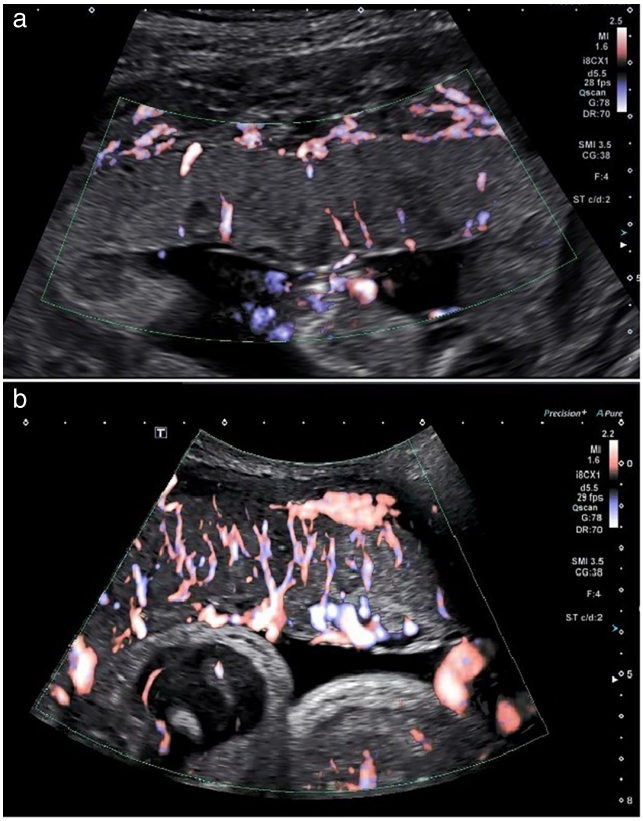


Figure 1 Superb microvascular imaging of first-trimester (a) and third-trimester (b) placenta, showing spiral arteries.

Descriptive statistics were reported and analyzed using chi-square or Fisher's exact test where appropriate for categorical data and continuous data were analyzed using Student's *t*-test. Pearson's correlation coefficient was calculated to assess the relationship between maternal SA- and UtA-PI across gestational timepoints. The longitudinal changes in maternal UtA-PI, SA-PSV and SA-PI were analyzed using mixed-effects analysis with Greenhouse–Geisser correction to determine whether there were any differences between the groups at any of the timepoints listed. The PI was calculated as the average of two measurements (right and left). PSV was calculated by averaging measurements in the central, lower and fundal locations. Distribution of response variables (Doppler) were assessed with quantile–quantile plots, skewness and kurtosis values. Doppler values were found to be right-skewed across gestational age and were log transformed to achieve normality of the residuals. Response variables were modeled as a function of gestational age and linear mixed-effects regression with natural cubic splines were employed. Candidate models were compared with likelihood ratio tests. Model intercepts were allowed to vary between different individuals and slopes were allowed to vary for the measurements of the same individual. Mean curve and standard deviation were estimated separately using the approach suggested by Royston and Wright[16]. All models were checked for outliers, influential data points, normality of residuals and absence of autocorrelation in residuals. Outliers were either kept or removed from the model after double-checking the veracity of the measurements. Model fit was assessed as described by Royston and Wright[17] by checking the normality of estimated *Z*-scores across the fitted range and independency from gestational age. *P*-values of < 0.05 were considered to be statistically significant. Statistical analyses were performed using SAS 9.4 software (SAS Institute Inc., Cary, NC, USA), GraphPad Prism 9.3.1 (GraphPad Software, San Diego, CA, USA) and R for Statistical Computing software (version 4.2.2; https://www.r-project.org/).

RESULTS

A total of 610 women were enrolled in the Human Placenta Project between 2016 and 2020. There were 90 women who fulfilled the study criteria and were included

© 2023 The Authors. *Ultrasound in Obstetrics & Gynecology* published by John Wiley & Sons Ltd on behalf of International Society of Ultrasound in Obstetrics and Gynecology.

14690705, 2023, 6, Downloaded from https://obgyn.onlinelibrary.wiley.com/doi/10.1002/uog.26312 by Koc University, Wiley Online Library on [26/02/2024]. See the Terms and Conditions (https://onlinelibrary.wiley.com/terms-and-conditions) on Wiley Online Library for rules of use; OA articles are governed by the applicable Creative Commons License

in the analysis. From these 90 women, 674 measurements were included in the construction of reference ranges. Summary statistics for each Doppler variable, stratified by gestational-age window are available in Table S1. Maternal demographics and placental location are described in Table 1. Maternal UtA-PI decreased throughout the first half of pregnancy from a mean of 1.39 ± 0.50 at 12–13 weeks' gestation to 0.88 ± 0.24 at 20–21 weeks and 0.69 ± 0.17 at 36–37 weeks' gestation (Figure 2a, Table S1). The mean number of SA visualized in a sagittal plane of the placenta increased from 8.83 ± 2.37 in the first trimester (12–13 weeks) to 16.99 ± 3.31 in the late-third trimester (36–37 weeks) (Table S2). The mean SA-PI was 0.57 ± 0.12 in the first trimester and decreased progressively during the second trimester, reaching a nadir of 0.40 ± 0.10 at 24–25 weeks, remaining relatively constant until the end of pregnancy (Figure 2b, Table S1). SA-PSV was highest in early pregnancy with a mean of 57.16 ± 14.84 cm/s at 12–13 weeks' gestation and continued to trend downward for the remainder of pregnancy reaching a nadir of 34.50 ± 15.08 cm/s at 36–37 weeks' gestation (Figure 2c, Table S1).

A statistically significant association was noted between changes in SA-PI and UtA-PI ($r = 0.5633$; $P < 0.001$) (Figure S1). There was no difference in SA-PI values based on SA location at any gestational age except at 28–29 weeks' gestation when lower uterine segment SA-PIs were noted to be lower compared to fundal measurements (0.375 *vs* 0.429; $P = 0.0198$) (Figure S2). There was no difference in SA-PSV based on SA location at any gestational age except 16–17 weeks' gestation when mean central SA-PSV was decreased compared to lower uterine segment SA-PSV (61.10 *vs* 51.35 cm/s; $P = 0.0330$) (Figure S3). These differences were deemed inconsequential and reference ranges for SA Doppler values were calculated using the measured central SA-PI values for practicality purposes. Multilevel regression models used to create reference ranges for SA-PSV and SA-PI in our normal pregnant population for given gestational ages are presented in Tables 2 and 3, respectively. Multilevel regression models used to create reference ranges for UtA-PI in our normal pregnancy population for given gestational ages are presented in Table S3. An online calculator for estimating percentile values was constructed and is available online at https://epsilonkappa.shinyapps.io/SMI_reference_tools/.

Table 1 Maternal demographic characteristics and placental location in a cohort of normal pregnancies ($n = 90$)

Parameter	*Value*
Age (years)	25.52 ± 4.08
Height (cm)	163.30 ± 7.95
Weight (kg)	63.73 ± 10.36
Body mass index (kg/m^2)	23.62 ± 3.20
Race	
Caucasian	39 (43.3)
Black/African American	50 (55.6)
Other	1 (1.1)
Ethnicity	
Hispanic/Latino/Latina	7 (7.8)
Non-Hispanic/Latino/Latina	83 (92.2)
Placental location	
Anterior	45 (50.0)
Posterior	38 (42.2)
Right lateral	1 (1.11)
Left lateral	1 (1.11)
Not reported	5 (5.55)

Data are given as mean ± SD or *n* (%).

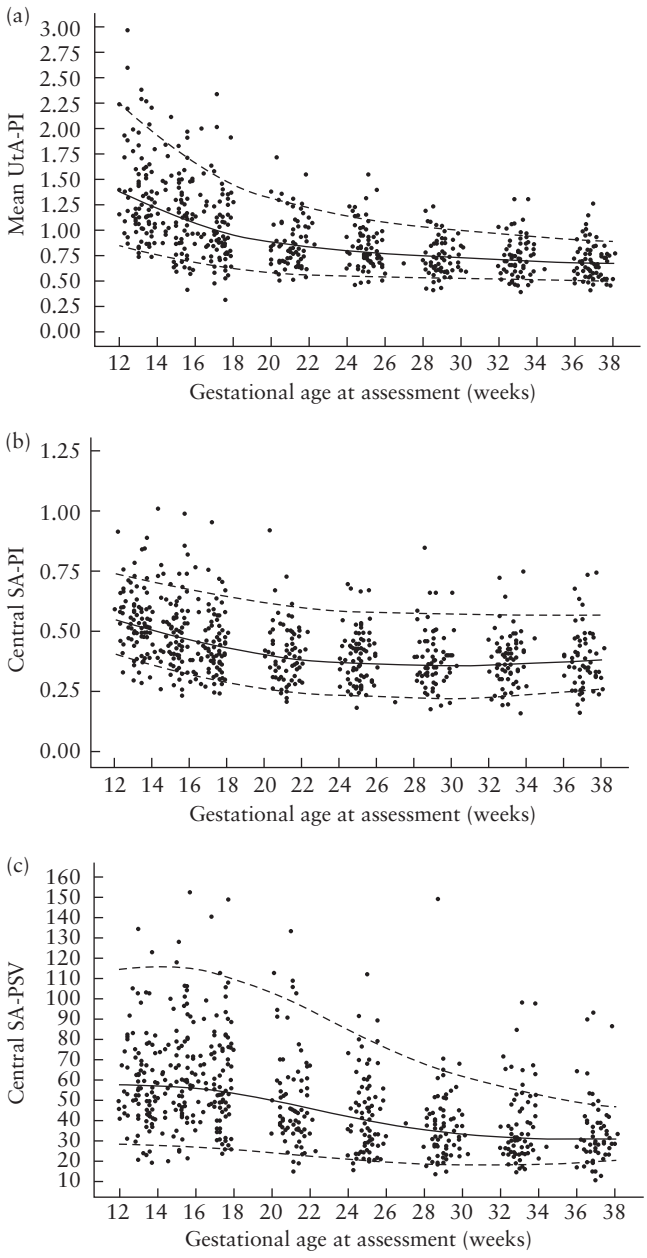


Figure 2 Scatterplots showing uterine artery pulsatility index (UtA-PI) (a), spiral artery pulsatility index (SA-PI) (b) and spiral artery peak systolic velocity (SA-PSV) (c), according to gestational age, in normal pregnancies. The 50th (——) and 2.5th and 97.5th (- - -) percentiles are shown.

© 2023 The Authors. *Ultrasound in Obstetrics & Gynecology* published by John Wiley & Sons Ltd on behalf of International Society of Ultrasound in Obstetrics and Gynecology.

14690705, 2023, 6, Downloaded from https://obgyn.onlinelibrary.wiley.com/doi/10.1002/uog.26312 by Koc University, Wiley Online Library on [26/02/2024]. See the Terms and Conditions (https://onlinelibrary.wiley.com/terms-and-conditions) on Wiley Online Library for rules of use; OA articles are governed by the applicable Creative Commons License

Table 2 Central spiral artery peak systolic velocity percentiles according to gestational age (GA), from 12–38 weeks' gestation, in normal singleton pregnancies

GA (weeks)	Percentile								
	3rd	5th	10th	25th	Median	75th	90th	95th	97th
12	29.15	31.70	36.06	44.73	56.83	72.21	89.57	101.90	110.80
13	28.90	31.46	35.85	44.61	56.87	72.50	90.21	102.81	111.93
14	28.62	31.19	35.61	44.42	56.78	72.59	90.55	103.36	112.63
15	28.27	30.84	35.24	44.05	56.44	72.31	90.39	103.30	112.65
16	27.78	30.32	34.68	43.41	55.72	71.51	89.52	102.39	111.74
17	27.14	29.62	33.91	42.49	54.59	70.14	87.89	100.60	109.82
18	26.37	28.80	32.97	41.33	53.13	68.31	85.64	98.04	107.05
19	25.53	27.87	31.91	40.00	51.42	66.11	82.87	94.88	103.59
20	24.63	26.89	30.77	38.56	49.53	63.64	79.73	91.25	99.61
21	23.71	25.88	29.60	37.05	47.54	61.00	76.35	87.33	95.29
22	22.81	24.87	28.42	35.52	45.50	58.28	72.83	83.22	90.75
23	21.93	23.90	27.27	34.01	43.47	55.56	69.28	79.07	86.16
24	21.11	22.98	26.19	32.57	41.51	52.90	65.80	74.98	81.61
25	20.37	22.14	25.18	31.23	39.66	50.36	62.45	71.03	77.22
26	19.71	21.39	24.28	30.00	37.95	48.00	59.30	67.30	73.07
27	19.15	20.76	23.50	28.91	36.40	45.84	56.40	63.85	69.21
28	18.71	20.24	22.85	27.99	35.06	43.91	53.78	60.71	65.69
29	18.39	19.86	22.35	27.23	33.92	42.24	51.47	57.93	62.55
30	18.22	19.63	22.01	26.67	33.01	40.85	49.49	55.51	59.81
31	18.17	19.53	21.82	26.27	32.30	39.70	47.80	53.41	57.41
32	18.24	19.55	21.76	26.02	31.75	38.74	46.33	51.57	55.28
33	18.41	19.68	21.81	25.90	31.34	37.94	45.05	49.92	53.37
34	18.68	19.91	21.96	25.88	31.05	37.26	43.90	48.43	51.62
35	19.03	20.22	22.20	25.94	30.84	36.67	42.86	47.05	49.98
36	19.47	20.61	22.51	26.07	30.70	36.16	41.88	45.74	48.43
37	19.97	21.07	22.88	26.26	30.61	35.67	40.95	44.47	46.91
38	20.54	21.59	23.30	26.49	30.54	35.21	40.02	43.20	45.41

Table 3 Central spiral artery pulsatility index percentiles according to gestational age (GA), from 12–38 weeks' gestation, in normal singleton pregnancies

GA (weeks)	Percentile								
	3rd	5th	10th	25th	Median	75th	90th	95th	97th
12	0.41	0.43	0.45	0.49	0.55	0.60	0.66	0.70	0.72
13	0.39	0.40	0.42	0.47	0.52	0.58	0.64	0.68	0.71
14	0.36	0.38	0.40	0.45	0.50	0.56	0.63	0.67	0.69
15	0.34	0.36	0.38	0.43	0.48	0.54	0.61	0.65	0.68
16	0.32	0.34	0.36	0.41	0.46	0.53	0.59	0.64	0.66
17	0.31	0.32	0.34	0.39	0.45	0.51	0.58	0.62	0.65
18	0.29	0.31	0.33	0.37	0.43	0.49	0.56	0.60	0.64
19	0.28	0.29	0.32	0.36	0.42	0.48	0.55	0.59	0.62
20	0.27	0.28	0.30	0.35	0.40	0.47	0.54	0.58	0.61
21	0.26	0.27	0.29	0.34	0.39	0.46	0.52	0.57	0.60
22	0.25	0.26	0.29	0.33	0.38	0.45	0.52	0.56	0.59
23	0.24	0.26	0.28	0.32	0.38	0.44	0.51	0.55	0.58
24	0.24	0.25	0.27	0.32	0.37	0.43	0.50	0.55	0.58
25	0.23	0.25	0.27	0.31	0.37	0.43	0.50	0.54	0.57
26	0.23	0.24	0.27	0.31	0.36	0.42	0.49	0.54	0.57
27	0.23	0.24	0.26	0.30	0.36	0.42	0.49	0.53	0.56
28	0.23	0.24	0.26	0.30	0.36	0.42	0.49	0.53	0.56
29	0.23	0.24	0.26	0.30	0.36	0.42	0.48	0.53	0.56
30	0.23	0.24	0.26	0.30	0.36	0.42	0.48	0.53	0.56
31	0.23	0.24	0.26	0.30	0.36	0.42	0.48	0.53	0.56
32	0.23	0.24	0.27	0.31	0.36	0.42	0.48	0.53	0.56
33	0.23	0.25	0.27	0.31	0.36	0.42	0.48	0.53	0.56
34	0.24	0.25	0.27	0.31	0.36	0.42	0.48	0.52	0.55
35	0.24	0.26	0.28	0.32	0.36	0.42	0.48	0.52	0.55
36	0.25	0.26	0.28	0.32	0.37	0.42	0.48	0.52	0.55
37	0.25	0.26	0.28	0.32	0.37	0.43	0.48	0.52	0.55
38	0.26	0.27	0.29	0.33	0.37	0.43	0.48	0.52	0.54

© 2023 The Authors. *Ultrasound in Obstetrics & Gynecology* published by John Wiley & Sons Ltd on behalf of International Society of Ultrasound in Obstetrics and Gynecology.

14690705, 2023, 6, Downloaded from https://obgyn.onlinelibrary.wiley.com/doi/10.1002/uog.26312 by Koc University, Wiley Online Library on [26/02/2024]. See the Terms and Conditions (https://onlinelibrary.wiley.com/terms-and-conditions) on Wiley Online Library for rules of use; OA articles are governed by the applicable Creative Commons License

DISCUSSION

In this study, we were able to demonstrate the ability of a novel ultrasound tool to image placental microvasculature from early pregnancy. We were also able to confirm longitudinal changes in the maternal placental vessels that reflect the placental adaptation in pregnancy. Indeed, SA-PI decreased progressively from the first trimester onward and reached a nadir at around 24 weeks, implying that placental adaptation is near complete by around this gestational age. This finding is consistent with those of previous studies examining longitudinal uteroplacental vascular adaptation in pregnancy using conventional Doppler[18]. Furthermore, SA-PSV decreased progressively from early gestation, further reflecting on the drop in peak vessel systolic pressure, which is essential to protect the integrity of the developing placental villi structure. Our noted linear increase in the number of SA imaged with gestational age may be a reflection of placental growth and adaptation, but also may result from improved imaging with increase in placental mass with advancing gestation.

Although previous studies have assessed UtA and SA Doppler indices during pregnancy[19–21], this study is unique in that we obtained Doppler measurements longitudinally, starting in the first trimester, and for a total of eight measurements per patient throughout pregnancy. A study by Deurloo *et al.*[22] examining longitudinal UtA and SA Doppler waveforms in nulliparous women without fetal anomalies, FGR or hypertensive disorders using transabdominal color Doppler ultrasound found a continuous decrease in mean UtA- and SA-PI from the first trimester to 24 weeks' gestation, which is consistent with our findings. Odibo *et al.*[14] demonstrated using SMI that the SA resistance index was increased in the third trimester in pregnancies that developed FGR or PE when compared to pregnancies that did not. The authors measured SA resistance index once per trimester and noted a difference only in the third trimester, but did not generate reference ranges.

We have noted a close correlation between the change in Doppler indices of the UtA and the SA in our normal pregnancy cohort. The changes seen in the UtA waveform during pregnancy have been historically attributed to trophoblast-induced remodeling of the SA altering the downstream vascular resistance[23]. However, this does not account for the fact that UtA waveforms have been observed to change in the absence of trophoblastic invasion, such as during the menstrual cycle, with intrauterine contraceptive devices and in extrauterine pregnancies, which suggests a possible link between hormonal changes and maternal uterine vascular tone[23]. Many historical models do not account for the presence of the arteriovenous anastomoses in the myometrium of the placental bed[23].

Until now, our ability to assess the human placenta non-invasively throughout pregnancy has been limited by conventional ultrasound technology. As ultrasound technology continues to evolve and our ability to evaluate the pathophysiologic processes that occur during abnormal placental development in early gestation improves, knowledge of normal values of maternal placental vasculature for gestational age is paramount to both identify pregnancies affected by abnormal uterine vascular adaptation and to guide future development of targeted therapies.

This study demonstrates that SA-PI and -PSV measurements are largely unaffected by SA sample location, as we assessed SA-PI and -PSV in three placental segments and documented no significant change overall with the exception of a single gestational window, which is most probably a statistical variation, rather than a physiologic change. Our finding is consistent with a 2020 meta-analysis examining SA blood flow during pregnancy which found no difference in SA-PI by SA location[24]. Interrogating the SA in the central portion of the placenta is therefore recommended, as it is commonly its thickest portion and thus easier technically. Whether Doppler abnormalities of SA in complicated pregnancies show similar findings between placental segments remains to be seen. We suggest the use of a cut-off of $> 95^{th}$ percentile for mean SA-PSV and -PI at a given gestational age, but this will need to be confirmed by studies which include complicated pregnancy with adverse outcome.

This study has several strengths. It is a large prospective study with longitudinal collection of data from eight ultrasound examinations at predefined timepoints throughout pregnancy. Ultrasound data points were acquired by skilled sonographers following additional training and certification in SA imaging and quantification of blood flow using SMI technology, following a standardized approach to the evaluation of the placenta. Furthermore, our strict selection criteria for our normal cohort ensure that the nomogram is reflective of maternal vascular adaptation in normal pregnancies. Imaging of SA using SMI and quantification of SA Doppler waveforms require expertise and training, which may represent a limitation to the wide applicability of our findings.

In conclusion, we have demonstrated the ability to image and quantify SA blood flow in normal pregnancy, starting from early gestation, and have developed reference ranges for use at various gestational ages throughout pregnancy.

ACKNOWLEDGMENT

The Human Placenta Project study (HD 086313-01) was funded by the National Institutes of Health (NIH).

REFERENCES

1. Brosens I, Pijnenborg R, Vercruysse L, Romero R. The "Great Obstetrical Syndromes" are associated with disorders of deep placentation. *Am J Obstet Gynecol* 2011; **204**: 193–201.
2. Espinoza J, Romero R, Mee Kim Y, Kusanovic JP, Hassan S, Erez O, Gotsch F, Than NG, Papp Z, Jai Kim C. Normal and abnormal transformation of the spiral arteries during pregnancy. *J Perinat Med* 2006; **34**: 447–458.
3. Lyall F, Robson SC, Bulmer JN. Spiral artery remodeling and trophoblast invasion in preeclampsia and fetal growth restriction: relationship to clinical outcome. *Hypertension* 2013; **62**: 1046–1054.
4. Gebb J, Dar P. Colour Doppler ultrasound of spiral artery blood flow in the prediction of pre-eclampsia and intrauterine growth restriction. *Best Pract Res Clin Obstet Gynaecol* 2011; **25**: 355–366.

© 2023 The Authors. *Ultrasound in Obstetrics & Gynecology* published by John Wiley & Sons Ltd on behalf of International Society of Ultrasound in Obstetrics and Gynecology.

14690705, 2023, 6, Downloaded from https://obgyn.onlinelibrary.wiley.com/doi/10.1002/uog.26312 by Koc University, Wiley Online Library on [26/02/2024]. See the Terms and Conditions (https://onlinelibrary.wiley.com/terms-and-conditions) on Wiley Online Library for rules of use; OA articles are governed by the applicable Creative Commons License

5. Collins SL, Birks JS, Stevenson GN, Papageorghiou AT, Noble JA, Impey L. Measurement of spiral artery jets: general principles and differences observed in small-for-gestational-age pregnancies. *Ultrasound Obstet Gynecol* 2012; **40**: 171–178.
6. Saghian R, James JL, Tawhai MH, Collins SL, Clark AR. Association of Placental Jets and Mega-Jets With Reduced Villous Density. *J Biomech Eng* 2017; **139**: 0510011–05100110.
7. Burton GJ, Jauniaux E. Pathophysiology of placental-derived fetal growth restriction. *Am J Obstet Gynecol* 2018; **218**: S745–761.
8. Deurloo KL, Spreeuwenberg MD, Bolte AC, Van Vugt JM. Color Doppler ultrasound of spiral artery blood flow for prediction of hypertensive disorders and intra uterine growth restriction: a longitudinal study. *Prenat Diagn* 2007; **27**: 1011–1016.
9. Machado P, Forsberg F. Initial experience with a novel microvascular flow imaging technique. *Toshiba Medical Systems Corporation* 2014. http://medical.toshiba.com/downloads/aplio-500-wp-tju-smi.pdf.
10. Hata J. Seeing the Unseen: New Techniques in Vascular Imaging. *Toshiba Medical Systems Corporation* 2018. http://medical.toshiba.com/downloads/aplio-500-wp-smi-seeing-the-unseen.
11. Kong J, Li JC, Wang HY, Wang YH, Zhao RN, Zhang Y, Jin J. Role of Superb Micro-Vascular Imaging in the Preoperative Evaluation of Thyroid Nodules: Comparison With Power Doppler Flow Imaging. *J Ultrasound Med* 2017; **36**: 1329–1337.
12. Park AY, Seo BK, Cha SH, Yeom SK, Lee SW, Chung HH. An Innovative Ultrasound Technique for Evaluation of Tumor Vascularity in Breast Cancers: Superb Micro-Vascular Imaging. *J Breast Cancer* 2016; **19**: 210–213.
13. Machado P, Segal S, Lyshchik A, Forsberg F. A Novel Microvascular Flow Technique: Initial Results in Thyroids. *Ultrasound Q* 2016; **32**: 67–74.
14. Odibo AO, Kayisli U, Lu Y, Kayisli O, Schatz F, Odibo L, Chen H, Bronsteen R, Lockwood CJ. Longitudinal assessment of spiral artery and intravillous arteriole blood flow and adverse pregnancy outcome. *Ultrasound Obstet Gynecol* 2022; **59**: 350–357.
15. Bhide A, Acharya G, Baschat A, Bilardo CM, Brezinka C, Cafici D, Ebbing C, Hernandez-Andrade E, Kalache K, Kingdom J, Kiserud T, Kumar S, Lee W, Lees C, Leung KY, Malinger G, Mari G, Prefumo F, Sepulveda W, Trudinger B. ISUOG Practice Guidelines (updated): use of Doppler velocimetry in obstetrics. *Ultrasound Obstet Gynecol* 2021; **58**: 331–339.
16. Royston P, Wright EM. A Method for Estimating Age-Specific Reference Intervals ('Normal Ranges') Based on Fractional Polynomials and Exponential Transformation. *J R Stat Soc Ser A Stat Soc* 1998; **161**: 79–101.
17. Royston P, Wright EM. Goodness-of-fit statistics for age-specific reference intervals. *Stat Med* 2000; **19**: 2943–2962.
18. Cohen-Overbeek T, Pearce JM, Campbell S. The antenatal assessment of utero-placental and feto-placental blood flow using Doppler ultrasound. *Ultrasound Med Biol* 1985; **11**: 329–339.
19. Flo K, Wilsgaard T, Acharya G. A new non-invasive method for measuring uterine vascular resistance and its relationship to uterine artery Doppler indices: a longitudinal study. *Ultrasound Obstet Gynecol* 2011; **37**: 538–542.
20. Hüneke B, Holst A, Schröder HJ, Carstensen MH. [Normal values for relative Doppler indices. A/B ratio, resistance index and pulsatility index of the uterine artery and umbilical artery in normal pregnancy. A longitudinal study]. *Geburtshilfe Frauenheilkd* 1995; **55**: 616–622.
21. Khalil A, Garcia-Mandujano R, Maiz N, Elkhouli M, Nicolaides KH. Longitudinal changes in uterine artery Doppler and blood pressure and risk of pre-eclampsia. *Ultrasound Obstet Gynecol* 2014; **43**: 541–547. Erratum in: Ultrasound Obstet Gynecol. 2014 Aug;44(2):244. Elkhaouli, M [corrected to Elkhouli, M].
22. Deurloo KL, Bolte AC, Twisk JW, van Vugt JM. Longitudinal Doppler measurements of spiral artery blood flow in relation to uterine artery blood flow. *J Ultrasound Med* 2009; **28**: 1623–1628.
23. Lloyd-Davies C, Collins SL, Burton GJ. Understanding the uterine artery Doppler waveform and its relationship to spiral artery remodelling. *Placenta* 2021; **105**: 78–84.
24. Schiffer V, Evers L, de Haas S, Ghossein-Doha C, Al-Nasiry S, Spaanderman M. Spiral artery blood flow during pregnancy: a systematic review and meta-analysis. *BMC Pregnancy Childbirth* 2020; **20**: 680.

SUPPORTING INFORMATION ON THE INTERNET

The following supporting information may be found in the online version of this article:

Figure S1 Correlation between spiral artery (SA) pulsatility index (PI) and uterine artery (UA) PI, according to gestational age.

Figure S2 Longitudinal changes in spiral artery (SA) pulsatility index (PI) by SA location, according to gestational age.

Figure S3 Longitudinal changes in spiral artery (SA) peak systolic velocity (PSV) by SA location, according to gestational age.

Table S1 Summary statistics for mean uterine artery pulsatility index, spiral artery pulsatility index and peak systolic velocity

Table S2 Longitudinal assessment of spiral artery number using superb microvascular imaging

Table S3 Uterine artery pulsatility index percentiles for lower, higher and mean measurements

© 2023 The Authors. *Ultrasound in Obstetrics & Gynecology* published by John Wiley & Sons Ltd on behalf of International Society of Ultrasound in Obstetrics and Gynecology.

14690705, 2023, 6, Downloaded from https://obgyn.onlinelibrary.wiley.com/doi/10.1002/uog.26312 by Koc University, Wiley Online Library on [26/02/2024]. See the Terms and Conditions (https://onlinelibrary.wiley.com/terms-and-conditions) on Wiley Online Library for rules of use; OA articles are governed by the applicable Creative Commons License